Macrobicyclic Tris(catecholate ligand) Complexes: Spectroscopy, Electrochemistry, and the Structure of $K_2[(H_2\text{-bicappedTRENCAM})MoO_2]$

Markus Albrecht, Sonya J. Franklin, and Kenneth N. Raymond*

Department of Chemistry, University of California, Berkeley, California 94720

Received February 9, 1994®

The coordination chemistry of the macrobicyclic triscatecholate ligands bicappedTRENCAM (**2**), bicappedTPT-TRENCAM (**3**), and bicappedTPTCAM (**4**), as well as the new ligand TPTCAM (**5**), has been investigated with Fe^{3+}, V^{4+}, Ti^{4+}, and Ga^{3+}. UV–visible spectroscopy suggests that the Fe(III) and the V(IV) compounds possess pseudooctahedral geometry at the central metal atom. The electrochemistry of the vanadium complexes of the above ligands and some comparison compounds ($[VbicappedTRENCAM)]^{2-}$ (**19**), $[V(ETA)]^{2-}$ (**20**)) has been probed by cyclic voltammetry. An exemplary 4d metal complex, $[MoO_2(H_2\text{-bicappedTRENCAM})]^{2-}$ (**24**), has been prepared. As shown by the X-ray structure analysis of the dipotassium salt, this *cis*-MoO_2 complex is formed by coordination of the cation external to the macrobicyclic ligand. Crystal data for $MoK_2C_{36}H_{38}N_8O_{14}\cdot DMF\cdot 5H_2O$: space group $P2_1/c$ (No. 14), $a = 13.322(2)$ Å, $b = 14.252(2)$ Å, $c = 27.885(3)$ Å, $\beta = 103.11(1)°$, $V = 5.157(3)$ Å^3, and $Z = 4$.

Introduction

Because the tris(catechol) siderophore[1,2] enterobactin is such a good ligand for highly charged metal cations such as iron(III) ($\log K_f = 49$),[3] several analogs which model its coordination behavior have been proposed and studied.[4-12] Although no siderophores are known which have a macrobicyclic structure, an extension of this class of analogs is the macrobicyclic catecholate compounds, in which the metal binding cavity is formed by two capping backbones and three catechol groups.[4,5,12,13] In the uncoordinated ligands the catechol units might be expected to be highly predisposed toward metal binding.[11,14] Varying the ligand backbones, and therefore the cavity size, allows for the systematic study of the metal binding behavior and coordination geometry. Recent investigations in these laboratories showed that several 3d metal complexes (Ti^{4+}, V^{4+}, Fe^{3+}) of the ligand H_6-bicappedTRENCAM (**2**) exhibit unusual distorted trigonal prismatic geometry at the metal center,[12,13] whereas main group metal complexes (Al^{3+}, Ga^{3+}) prefer octahedral coordination geometry.[13] This behavior was attributed to the influence of π-bonding involving the partially filled 3d shells of the metal ions. The iron(III) complex of the larger H_6-bicappedTPTCAM (**4**), however, exhibits the more usual octahedral geometry,[13] in contrast to the other 3d metal complexes of **2**.

The purpose of the present study is to investigate the coordination behavior of transition metals with the macrobicyclic ligands **2**–**4**. These ligands show a stepwise increase in the available metal-binding cavity size with successive variation of the linking groups capping the three 2,3-dihydroxy terephthalamide units. This work focuses on the syntheses of metal complexes of **2**–**4** and the influence of ligand size on the electronic spectra and electrochemistry of the complex. The coordination chemistry of the new monocapped ligand H_6-TPTCAM (**5**), and the bidentate ligands H_2-ETA (**6a**)[8] and H_2-BTA (**6b**)[8] are presented for comparison. In contrast to the encapsulation of the relatively small, isotropic ions Ga^{3+}, Ti^{4+}, V^{4+}, and Fe^{3+}, the cage molecule **2** coordinates the larger, more complex cation MoO_2^{2+} external to the cavity. Compounds **1**–**6** are shown in Chart 1.

Experimental Section

The metal complexes are stable when exposed to air; nevertheless the syntheses were performed under argon using degassed solvents. The ligand TREN (tris-(2-aminoethyl)amine, W. R. Grace and Co.) was distilled from sodium spheres; TPT (tris-(3-aminopropyl)amine) was prepared according to published procedure starting with tris(2-cyanoethyl)amine;[15] (2,2′,2″-Tris(2,3-dimethoxyterephthalic (2-mercaptothiazolinamide))triamido)triethylamine,[13] H_6-bicappedTRENCAM·2HBr (**2**),[13] H_6-bicappedTPTCAM·2HBr (**3**),[13] H_2-ETA (**6a**),[16] and H_2-BTA (**6b**),[16] as well as $K_2[V(bicappedTRENCAM)]$ (**19**),[17] and $K_2[V(ETA)_3]$ (**20**)[16] were prepared as described in the literature. All other compounds were reagent grade and were not further purified.

^{1}H NMR spectra were measured at 298 K on a Bruker AM-400 or AM-500 spectrometer. Absorption spectra were recorded on a HP 8450 UV–visible spectrophotometer. IR spectra were recorded using a Nicolet 5DX FT IR spectrometer. Microanalyses were performed by the Analytical Services Laboratory, and FAB mass spectra by the Mass Spectrometry Laboratory, both of the College of Chemistry, University of California, Berkeley.

* To whom correspondence should be addressed.

® Abstract published in *Advance ACS Abstracts,* November 1, 1994.

(1) Matzanke, B. F.; Müller-Matzanke, G.; Raymond, K. N. In *Iron Carriers and Iron Proteins*; Loehr, T. M., Ed.; VCH Publishers: New York, 1989; p 1.
(2) Raymond, K. N. *Coord. Chem. Rev.* **1990**, *105*, 135.
(3) Loomis, L. D.; Raymond, K. N. *Inorg. Chem.* **1991**, *30*, 906.
(4) Kiggen, W.; Vögtle, F. *Angew. Chem., Int. Ed. Engl.* **1984**, *23*, 714.
(5) Stutte, P.; Kiggen, W.; Vögtle F. *Tetrahedron* **1987**, *43*, 2065.
(6) Coleman, A. W.; Ling, C.-C.; Miocque, M. *Angew. Chem., Int. Ed. Engl.* **1992**, *31*, 1381.
(7) Tse, B.; Kishi, Y. *J. Am. Chem. Soc.* **1993**, *115*, 7893.
(8) Garrett, T. M.; Miller, P. W.; Raymond, K. N. *Inorg. Chem.* **1989**, *28*, 128.
(9) Weitl, F. L.; Raymond, K. N. *J. Am. Chem. Soc.* **1979**, *101*, 2728.
(10) Rodgers, S. J.; Lee, C.-W.; Ng, C. Y.; Raymond, K. N. *Inorg. Chem.* **1987**, *26*, 1622.
(11) Stack, T. D. P.; Hou, Z.; Raymond, K. N. *J. Am. Chem. Soc.* **1993**, *115*, 6466.
(12) Garrett, T. M.; McMurry, T. J.; Hosseini, M. W.; Reyes, Z. E.; Hahn, F. E.; Raymond, K. N. *J. Am. Chem. Soc.* **1991**, *113*, 2965.
(13) Karpishin, T. B.; Stack, T. D. P.; Raymond, K. N. *J. Am. Chem. Soc.* **1993**, *115*, 182.
(14) Shanzer, A.; Libman, J.; Lifson, S.; Felder, C. E. *J. Am. Chem. Soc.* **1986**, *108*, 7609.
(15) Chin, J.; Banaszyzyk, M.; Jubian, V.; Zou X. *J. Am. Chem. Soc.* **1989**, *111*, 186.
(16) Dewey, T. M. Ph.D. Thesis, University of California, Berkeley, 1992.
(17) Karpishin, T. B.; Dewey, T. M.; Raymond, K. N. *J. Am. Chem. Soc.* **1993**, *115*, 1842.

0020-1669/94/1333-5785$04.50/0

Chart 1

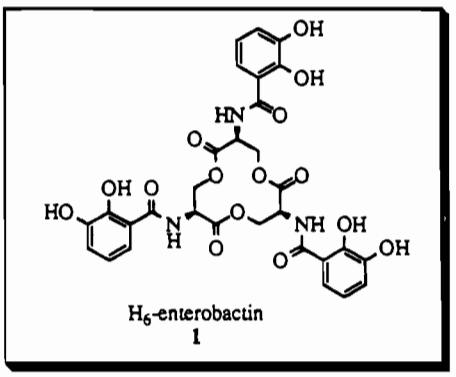

H_6-enterobactin
1

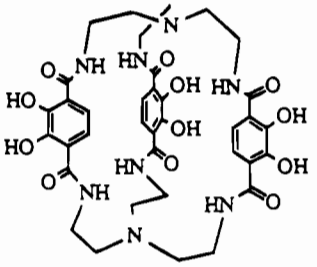

H_6-bicappedTRENCAM
2

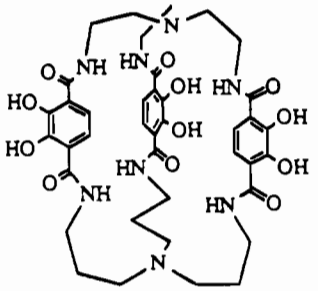

H_6-bicappedTPTTRENCAM
3

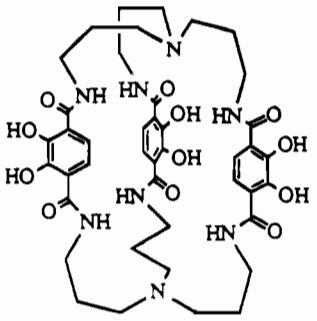

H_6-bicappedTPTCAM
4

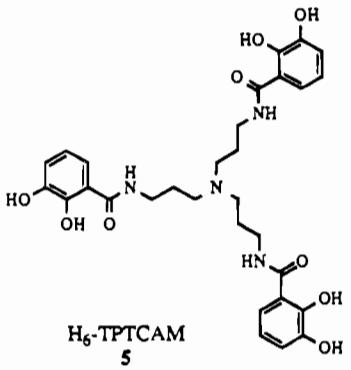

H_6-TPTCAM
5

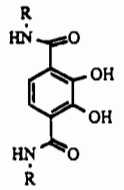

R = Et: H_2-ETA **6a**
R = Bu: H_2-BTA **6b**

Electrochemistry of Vanadium Compounds. Cyclic voltammograms were collected using a BAS 100A electrochemical analyzer. All potentials were measured at a scan rate of 0.1 V/s under an argon atmosphere using a platinum electrode. Potentials are reported relative to the saturated calomel electrode (SCE). Concentrations of the vanadium compounds were about 0.1 mM in 0.1 M Bu_4NPF_6/DMF. Under the same conditions, the Cp_2Fe/Cp_2Fe^+ potential was measured at 0.50 V with a peak separation of 67 mV.[18]

Me_6-BicappedTPTTRENCAM (8). A solution of (2,2′,2″-tris(2,3-dimethoxyterephthalic (2-mercaptothiazolinamide))triamido)triethylamine (2.033 g, 1.89 mmol) in 500 mL of methylene chloride and a solution of TPT (tripropylenetetramine) (0.353 g, 1.94 mmol) in 500 mL of methylene chloride (containing 1 mL of triethylamine and 10 mL of methanol) were added simultaneously (FMI pump; addition rate: 5 mL/h) to 3 L of vigorously stirring methylene chloride over the course of 5 days. After complete addition, the mixture was stirred overnight and solvent evaporated to 300 mL. The solution was washed with 0.1 M aqueous NaOH, dried over $MgSO_4$ and solvent was removed to yield an oil which was purified by chromatography over silica (2−12% methanol/methylene chloride). The macrobicyclic compound was obtained as a white solid (1.002 g, 1.12 mmol, 59%).

(18) Bard, A. J; Faulkner, L. R. *Electrochemical Methods*; Wiley: New York, 1980.

^{1}H NMR ($CDCl_3$/TMS, 500 MHz): δ 7.99, 7.95 (2 m, 3 H each), 7.51, 7.41 (2 d, J = 6.3 Hz, 3 H each), 3.63, 3.57 (2 m, 6 H each), 3.49, 3.42 (2 s, 9 H each), 2.78, 2.65, 1.79 ppm (3 m, 6 H each).

H_6-BicappedTPTTRENCAM·2HBr (3).[12] To **8** (242 mg, 0.27 mmol) in 30 mL of degassed methylene chloride at 0 °C, 2 mL of BBr_3 were added. The yellow suspension which immediately formed was stirred for 4 days at ambient temperature. Slow addition of water (a total of 200 mL), evaporation of methylene chloride and subsequent heating of the aqueous solution at reflux for several hours resulted in a brown solution. At 4 °C a brown wax precipitated. The wax was repeatedly dissolved in hot methanol and taken to dryness until a cream colored solid was formed, which was then recrystallized from methanol/ether to yield **3** as a gray-white solid (190 mg, 0.18 mmol, 67%; **3** is air sensitive, when wet).

^{1}H NMR (dmso-d_6, 400 MHz): δ 12.09, 11.69 (2 s, 3 H each), 9.72, 9.46 (2 m, 1 H each), 8.82, 8.68 (2 m, 3 H each), 6.94, 6.75 (2 d, J = 8.5 Hz, 3 H each), 3.79, 3.61, 3.41, 3.22, 2.00 ppm (5 m, 6 H each). Anal. Calcd (found) for $C_{39}H_{50}Br_2N_8O_{12}$·$CH_3OH$·$3H_2O$: C, 44.95 (45.16); H, 5.68 (5.53); N, 10.48 (10.39).

Me_6-TPTCAM (9). TPT (321 mg, 1.76 mmol) and 2,3-dimethoxybenzoic mercaptothiazolide (1.50 g, 5.29 mmol) were dissolved in 100 mL of CH_2Cl_2. The mixture was stirred for 5 h at which point no remaining mercaptothiazolide could be detected by tlc (silica, CH_2Cl_2:CH_3OH = 95:5). The organic layer was washed 3 times with 0.1 M

KOH, dried over $MgSO_4$ and taken to dryness. The remaining oil (one spot on tlc) was used without further purification.

^1H NMR spectrum ($CDCl_3$, 400 MHz): δ 8.02 (m, 3 H), 7.60 (dd, J = 1.6, 8.0 Hz, 3 H), 7.11 (pseudo t, J = 8.0 Hz, 3 H), 7.00 (dd, J = 1.6, 8.0 Hz, 3 H), 3.87 (s, 18 H), 3.48, 2.54, 1.76 ppm (3 m, 6 H each).

H_6-TPTCAM·HBr (5).[12] The oil **9** was dissolved in 50 mL of CH_2Cl_2 under argon and 3 mL of BBr_3 were added. The yellow suspension was stirred at ambient temperature for 3 days. Volatiles were removed under vacuum. The residue was quenched with methanol, taken to dryness, and heated at reflux in water for 2 h. After cooling the solution to ambient temperature, the waxy precipitate was collected. This solid was resuspended in methanol or ether and solvent removed several times to yield the beige solid **5** (627 mg, 54%).

^1H NMR spectrum (400 MHz, dmso-d_6): δ 12.49 (s, 3 H), 9.20 (2 m, 4 H), 8.84 (m, 3 H), 7.24, 6.90, 6.67 (3 m, 3 H each), 3.34, 3.17, 1.91 ppm (3 m, 6 H). Anal. Calcd (found) for $C_{30}H_{37}BrN_4O_9 \cdot 0.5H_2O$: C, 52.48 (52.86); H, 5.58 (6.0); N, 8.16 (7.79).

K_3[(bicappedTPTTRENCAM)Fe] (10). To H_6-bicappedTPTTRENCAM·2HBr (**3**) (62 mg, 0.063 mmol) in 30 mL of methanol, first 0.636 mL of 0.5 M KOH/ethanol (0.318 mmol), and then iron (III) acetylacetonate (20 mg, 0.063 mmol) were added. The dark red mixture was stirred for 1 h and solvent was subsequently removed under vacuum. The residue was purified by chromatography (Sephadex LH-20, methanol). After evaporation of the solvent, the dark red solid **10** was obtained (58 mg, 0.054 mmol, 86%), which was recrystallized from wet DMF/ether.

IR (KBr): 2945, 1609, 1550, 1441, 1202 cm^{-1}. UV/vis spectrum (H_2O, pH = 7): λ_{max} 363 nm (ϵ = 8600 M^{-1} cm^{-1}), 444 nm (ϵ = 4900 M^{-1} cm^{-1}), 508 nm (ϵ = 4250 M^{-1} cm^{-1}). Negative ion FAB MS (NBA): m/e = 948 ($K_2[M]^-$, 25%), 910 ($K[HM]^-$, 100%), 872 ($[H_2M]^-$, 80%). Anal. Calcd (found) for $C_{39}H_{42}FeK_3N_8O_{12} \cdot 0.5(H_3C)_2NCHO \cdot 3H_2O$: C, 44.81 (44.80); H, 4.78 (5.69); N, 11.61 (11.99).

K_3[Fe(TPTCAM)] (11). The Fe(III) complex of **5** was made in an analogous fashion to the synthesis of **10**, yielding the dark red complex **11**.

UV/vis spectrum (H_2O, pH = 7): λ_{max} 333 nm (ϵ = 14000 M^{-1} cm^{-1}), 508 nm (ϵ = 3460 M^{-1} cm^{-1}).

K_2[(bicappedTPTTRENCAM)V] (12). H_6-bicappedTPTTRENCAM·2HBr (**3**) (60 mg, 0.061 mmol) was dissolved in 20 mL of methanol, to which 0.488 mL of 0.5 M KOH/ethanol (0.244 mmol) were added. After addition of vanadyl acetylacetonate (16 mg, 0.060 mmol) the solution initially turned green but gradually became dark blue. A drop of 1 M HBr was added and the mixture was heated at reflux overnight. After evaporation of solvent the residue was chromatographed (Sephadex LH-20, methanol) to yield dark blue **12** (53 mg, 0.051 mmol, 84%).

UV/vis spectrum (H_2O, pH = 7): λ_{max} 346 nm (ϵ = 10800 M^{-1} cm^{-1}), 450 nm, (ϵ = 6900 M^{-1} cm^{-1}), 584 nm (ϵ = 8550 M^{-1} cm^{-1}), 644 nm (ϵ = 8450 M^{-1} cm^{-1}). Negative ion FAB MS (NBA): m/e = 866 $[HM]^-$. Anal. Calcd (found) for $C_{39}H_{42}K_2N_8O_{12}V \cdot CH_3OH \cdot 4\ H_2O$: C, 45.84 (46.08); H, 5.19 (5.19); N, 10.69 (10.45).

K_2[(bicappedTPTCAM)V] (13). The vanadium complex of **4** was synthesized in an analogous fashion to compound **12**, yielding **13** as a dark blue solid (82%).

UV/vis spectrum (H_2O, pH = 7): λ_{max} 350 nm (ϵ = 9400 M^{-1} cm^{-1}), 448 nm (ϵ = 4700 M^{-1} cm^{-1}), 588 nm (ϵ = 6330 M^{-1} cm^{-1}). Negative ion MS (NBA): m/e = 908 $[HM]^-$. Anal. Calcd (found) for $C_{42}H_{48}K_2N_8O_{12}V \cdot 5H_2O$: C, 46.88 (46.37); H, 5.43 (5.01); N, 10.41 (10.11).

K_2[(TPTCAM)V] (14). The vanadium complex of **5** was synthesized as described for compound **12**, although the addition of HBr was omitted prior to heating at reflux. The dark blue product **14** was obtained in 91% yield.

UV/vis spectrum (H_2O, pH = 7) : λ_{max} 322, 440, 585 nm. Anal. Calcd (found) for $C_{30}H_{30}K_2N_4O_9V \cdot 2H_2O$: C, 47.68 (47.40); H, 4.53 (4.42); N, 7.41 (7.30).

K_2[(bicappedTPTTRENCAM)Ti] (15). To H_6-bicappedTPTTRENCAM·2HBr (**3**) (48 mg, 0.049 mmol) in 30 mL of methanol, first 0.392 mL of 0.5 M KOH/ethanol, and then $(acac)_2TiO$ (13 mg, 0.050 mmol) were added. After stirring overnight, the mixture was taken to dryness and the residue was purified by chromatography over Sephadex LH-20 (methanol) to yield **15** (41 mg, 0.039 mmol, 80%).

^1H NMR spectrum (400 MHz, dmso-d_6): δ 9.58, 9.05 (2 d, 3 H each), 7.06 (br., 6 H), 3.50, 3.38, 3.32, 2.92 , 1.71 ppm (5 m, each 6 H). UV/vis spectrum (H_2O, pH = 7): λ_{max} 399 nm (ϵ = 18000 M^{-1} cm^{-1}). Anal. Calcd (found) for $C_{39}H_{42}K_2N_8O_{12}Ti \cdot CH_3OH \cdot 4H_2O$: C, 45.98 (45.61); H, 5.21 (5.18); N, 10.72 (10.26).

K_2[(bicappedTPTCAM)Ti] (16). Compound **16** was synthesized from **4** *via* a method analogous to that for compound **15**. A broad single orange band was collected from the Sephadex column, which after evaporation of the solvent gave **16** in 50% yield.

^1H NMR spectrum (400 MHz, dmso-d_6): δ 8.92 (m, 6 H), 7.09 (s, 6 H), 3.31 (m, 12 H), 2.81 (m, 12 H), 1.63 ppm (m, 12 H). UV/vis spectrum (H_2O, pH = 7): λ_{max} 397 nm (ϵ = 17900 M^{-1} cm^{-1}). Negative ion MS (NBA): m/e = 905 ($[HM]^-$, 100 %), 943 ($K[M]^-$, 30%). Anal. Calcd (found) for $C_{42}H_{48}K_2N_8O_{12}Ti \cdot 4H_2O$: C, 47.82 (48.01); H, 5.35 (5.08); N, 10.62 (10.30).

K_3[(bicappedTPTTRENCAM)Ga] (17). H_6-bicappedTPTTRENCAM·2HBr (**3**) (57 mg, 0.058 mmol) was dissolved in methanol (30 mL) and 0.5 M KOH/ethanol (0.58 mL) was added. After addition of $Ga(acac)_3$ (19 mg, 0.057 mmol) the mixture was stirred overnight. Evaporation of solvent and chromatography (Sephadex LH-20/methanol) yielded **17** (53 mg, 85%).

^1H NMR spectrum (400 MHz, dmso-d_6): δ 11.05, 10.85 (2 m, 3 H each), 6.66 (br., 6 H), 3.39, 3.31, 2.93, 2.33, 1.63 ppm (4 m, 6 H each). Anal. Calcd (found) for $C_{39}H_{42}K_3N_8O_{12}Ga \cdot 4H_2O$: C, 43.62 (43.82); H, 4.69 (4.66); N, 10.43 (10.11).

K_3[(bicappedTPTCAM)Ga] (18). Compound **18** was synthesized from **4** in 78% yield *via* the method described for compound **17**.

^1H NMR spectrum (dmso-d_6, 500 MHz): δ 10.68 (m, 6 H), 6.71 (s, 6 H), 3.36, 2.82, 1.53 ppm (3 m, 12 H each). Anal. Calcd (found) for $C_{42}H_{48}K_3N_8O_{12}Ga \cdot CH_3OH \cdot 3H_2O$: C, 45.71 (45.36); H, 5.17 (4.89); N, 9.92 (9.42).

Na_2[(H_2-bicappedTRENCAM)MoO_2] (24). To H_6-bicappedTRENCAM·2HBr (**2**) (60 mg, 0.064 mmol) in 40 mL of methanol under argon, 0.64 mL of a 0.5 M KOH/ethanol solution (0.32 mmol) was added. The yellow solution which immediately formed was added to molybdenyl acetylacetonate (21 mg, 0.064 mmol) in 20 mL of methanol, at which point the mixture turned orange. After one hour at room temperature the mixture was acidified with 1 M aqueous HBr. At pH < 6 a grey-green solid precipitates, which is isolable at pH = 4, and was shown to be H_6-bicappedTRENCAM (**2**). Using 1 M NaOH (approximately 1 to 1.5 mL) and 1 M HBr, the pH of the mixture was adjusted as low as possible without precipitation (about 6) to obtain a clear orange solution. After evaporation of solvent the residue was applied to column (Sephadex LH-20, methanol) to obtain **24** as an orange solid (57 mg, 0.060 mmol, 94%) which was recrystallized from wet DMF/ether.

^1H NMR spectrum (D_2O, 400 MHz): δ 6.86 (s, 4 H), 5.25 (s, 2 H), 3.55, 3.26, 3.08, 2.89, 2.74, 2.54 ppm (6 m, 4 H each); (dmso-d_6, 400 MHz): 12.28 (s, 2 H), 9.27 (m, 4 H), 6.70 (s, 4 H), 6.33 (m, 2 H), 5.61 (s, 2 H), 3.33, 3.21, 2.70 ppm (3 m, 24 H). IR (KBr): 899, 863 cm^{-1} (*cis*-MoO_2). Negative ion FAB MS (TEA): m/e = 905 ($H[H_2M]^-$, 40%). UV/vis spectrum (H_2O, pH = 7): λ_{max} 370 nm (ϵ = 10650 M^{-1} cm^{-1}). Anal. Calcd for $C_{36}H_{38}MoN_8Na_2O_{14} \cdot 2(H_3C)_2NCHO \cdot 4H_2O$: C, 43.22 (43.13); H, 5.18 (5.32); N, 12.00 (11.94).

Na_2[($BTA)_2MoO_2$] (25). The dihydrate of sodium molybdate (50 mg, 0.21 mmol) was suspended in 5 mL of ethanol under argon. To this suspension a solution of H_2-BTA (**6b**) (199 mg, 0.65 mmol) in 15 mL of ethanol was added. The solution turned yellow-green and was stirred at ambient temperature for 2 h. After an additional two hours at reflux the solution became brown. The solvent was evaporated and the residue was applied to a column (silica; 5−20% methanol/methylene chloride). After evaporation of solvent an orange solid was obtained (130 mg, 0.17 mmol, 81%), which was recrystallized from wet DMF/ether.

^1H NMR spectrum (dmso-d_6, 400 MHz): δ 9.19 (m, 4 H), 6.95 (s, 4 H), 3.12 (m, 8 H), 1.20 (m, 16 H), 0.78 ppm (t, J = 7.1 Hz, 12 H). IR (KBr): 899, 864 cm^{-1} (*cis*-MoO_2). Negative ion FAB MS (NBA): m/e = 765 ($Na[M]^-$; 85%). Anal. Calcd (found) for $C_{32}H_{44}MoN_4Na_2O_{10} \cdot 2(H_3C)_2NCHO \cdot 1.5H_2O$: C, 47.55 (47.53); H, 6.41 (6.04); N, 8.76 (8.87).

Table 1. ^{1}H NMR Shifts of the Ligands **2**, **3**, and **4** (·2HBr), and the Ti (**15**, **16**), Ga (**17**, **18**), and Mo (**24**) Complexes in dmso-d_6

	2·2HBr	3·2HBr	4·2HBr	15	16	17	18	24
OH	11.75 (s)	12.09, 11.69 (2s)	12.82 (s)					12.28 (s)
N^+H	10.05 (s)	9.72, 9.46 (2s)	9.81 (s)					
NH_{amide}	8.93 (m)	8.82, 8.68 (2m)	8.87 (m)	9.58, 9.05 (2m)	8.92 (m)	11.05, 10.85 (2m)	10.68 (m)	9.27 (br, 4H)*, 6.33 (br, 2H)
CH_{aryl}	6.78 (s)	6.94, 6.75 (2d)) J = 8.5 Hz)	7.23 (s)	7.06 (br)	7.09 (s)	6.66 (br)	6.71 (s)	6.70 (s, 4H)*, 5.61 (s, 2H)
CH_{alkyl}	3.80, 3.73 (2m)	3.79, 3.61, 3.41, 3.22, 2.00 (5m)	3.47, 2.99, 1.94 (3m)	3.50, 3.38, 3.32, 2.92, 1.71 (5m)	3.31, 2.81, 1.63 (3m)	3.39, 3.31, 2.93, 2.33, 1.63 (5m)	3.36, 2.82, 1.53 (3m)	3.33, 3.21, 2.70 (3m)

* Coordinating catechol units!

Scheme 1

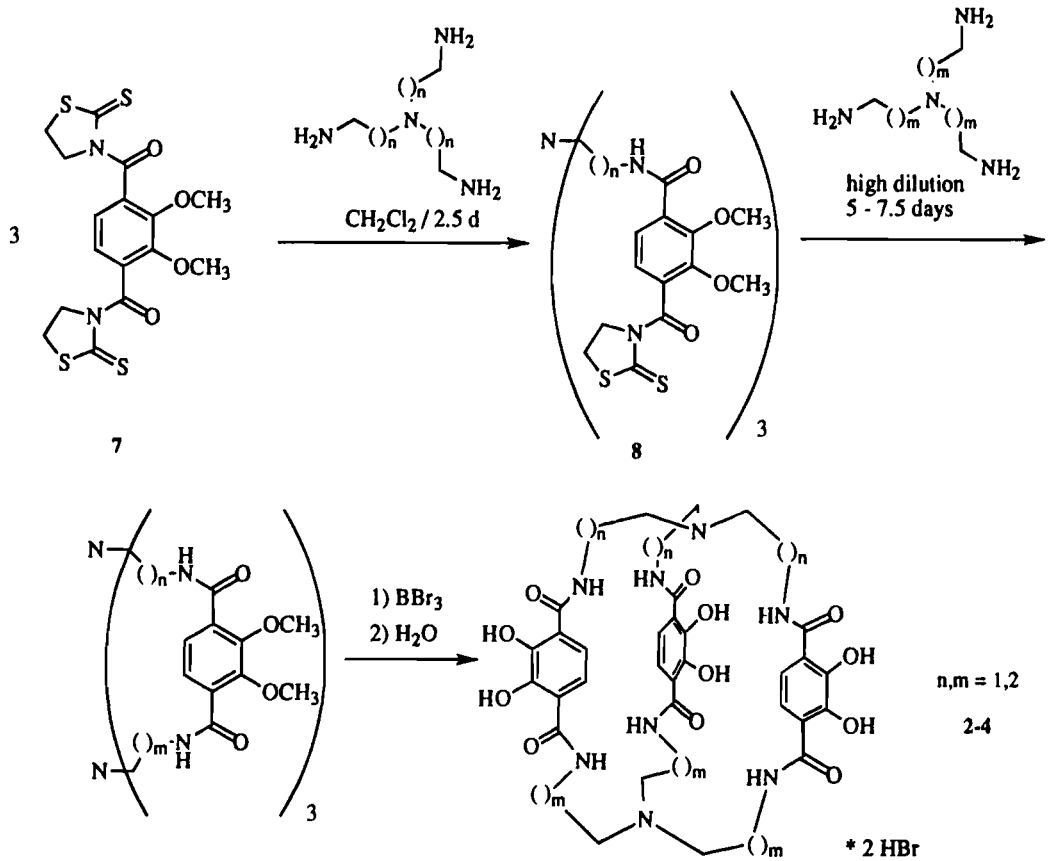

X-ray Diffraction. Bright orange plate-like crystals of compound **24′** were obtained from slow diffusion of ether into wet DMF from which a fragment was cut and mounted in Paratone. Data collection and cell parameters are summarized in Table 4. Intensity standards measured every 1 h of exposure time indicated no significant decomposition occurred during data collection. The same three reflections were checked against their predicted positions every 200 reflections and crystal orientation was redetermined if any of the three deviated by more then 0.1°. The crystal was reoriented once during the 36.2 h of exposure.

The structure was solved by Patterson methods. Refinement was performed on F, with a dampening factor of 0.7. Ligand hydrogen positions were predicted and included in the structure factor calculation, but not refined. The structure showed extreme disorder in the solvent and potassium counterions. Peaks attributed to DMF and water ran in well-defined channels approximately along the b axis. The disorder was modeled as two DMF molecules of 0.5 multiplicity and as nine oxygen positions with a total multiplicity of 5.35 oxygens. The thermal parameters of each of two groups of potassium ion fragments were constrained to be equal and the multiplicities of five positions refined to a total multiplicity of 1.983 potassium atoms. All partial occupancy atoms were refined isotropically. Prior to the final refinement, 16 reflections with abnormally large residual values were weighted to zero. The final residuals for 701 variables refined against 3272 data were R = 6.34 % and R_w = 7.23%, with GOF = 1.634.

Results and Discussion

Syntheses. The symmetric macrobicyclic ligands H_6-bicappedTRENCAM·2HBr (**2**) and H_6-bicappedTPTCAM·2HBr (**4**) were synthesized *via* the method[13] outlined in Scheme 1. The yields of the high dilution macrocyclizations (52% (**2**), 64% (**4**)) are extraordinarily high for this type of reaction. The unsymmetric ligand H_6-bicappedTPTTRENCAM·2HBr (**3**) containing one TREN and one TPT backbone was obtained in a similar fashion, with a 59% yield for the macrocyclization step. Metal complexes were obtained by the addition of the ligands **2**−**4** to appropriate metal compounds in methanol, followed by chromatographic workup (Sephadex LH-20, methanol).

^{1}H NMR Spectroscopy. The ^{1}H-NMR spectra of the ligands **2**−**4** (·2HBr) in dmso-d_6 show the high symmetry of the molecules (see Table 1). Compounds **2** and **4** each possess 3-fold symmetry (axis through the apical nitrogen atoms) and a mirror plane dividing the three catechol units. Ligand **3**, however, lacks this mirror symmetry because of its two different backbones, leading to the duplication of the 2,3-dihydroxy terephthalamide signals relative to **2** and **4**.[19]

In contrast to the paramagnetic Fe(III) and V(IV) complexes,[20,21] the Ti(IV) and Ga(III) complexes[22,23] can be studied

Scheme 2

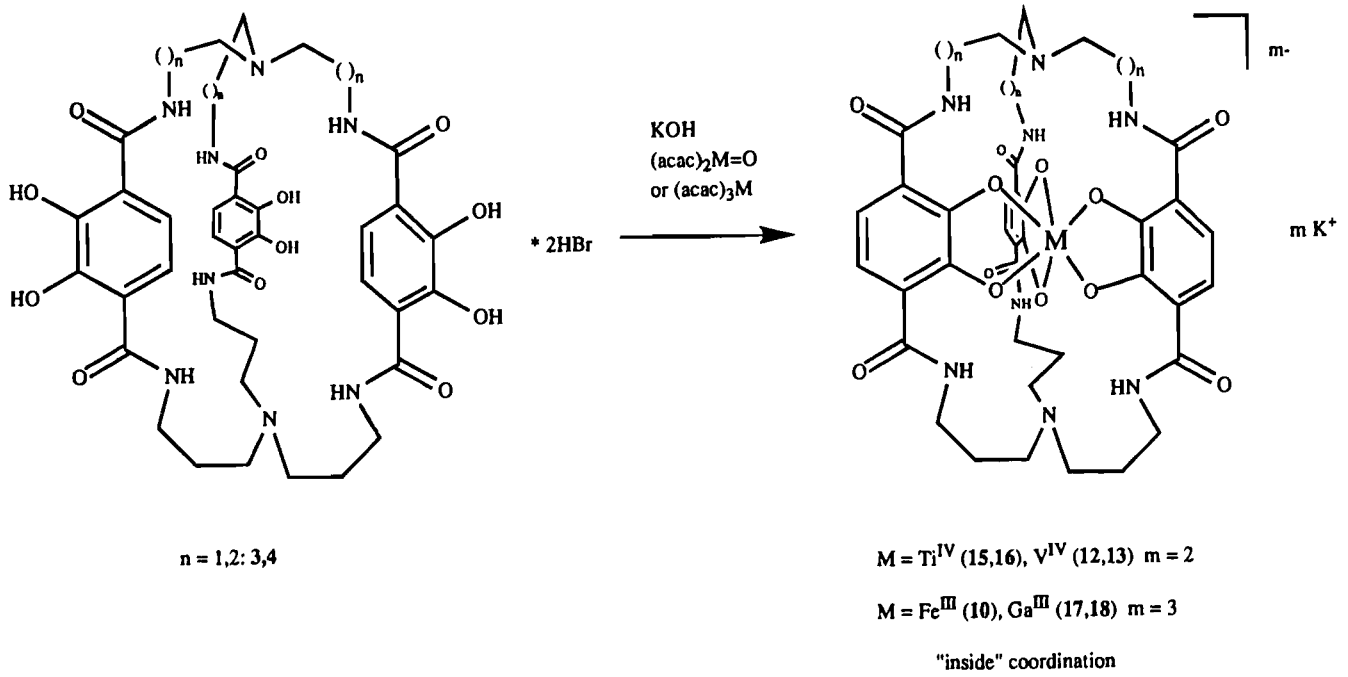

in detail by NMR; ^{1}H NMR shifts of the metal complexes **15** and **16** (Ti(IV)) and **17** and **18** (Ga(III)) in dmso-d_6, along with the shifts of the uncoordinated ligands **2**−**4** (·2HBr), are shown in Table 1. As observed in the ligand spectra, the compounds **16** and **18** show only one set of signals for the three catechol bisamide units, due to the 3-fold symmetry. In addition, mirror or inversion symmetry leads to equivalence of, for example, the amide protons of the terephthalamide units. Although they contain 3-fold symmetry, this further equivalence is not observed for the bicappedTPTTREN complexes (**15**, **17**), where two different amide signals are detected.

A further remarkable feature of the complex spectra is the downfield shift of the amide protons (up to 11.05 ppm in **17**) compared to the corresponding protons in the free ligands. This suggests hydrogen bridging between the amide nitrogen and the catecholate oxygen atoms that coordinate to the metal centers,[24] similar to that seen in other 2,3-dihydroxy terephthalamide complexes.[8,12,13,25,26] Although the ^{1}H NMR spectra are consistent with a highly symmetric environment in compounds **15**−**18**, no distinction between trigonal prismatic and octahedral geometry at the metal center can be made based on this spectroscopic method.

UV−Visible Spectroscopy. Recently it was shown that UV−visible spectroscopy of 2,3-dihydroxyterephthalamide complexes gives some indication of the geometry at the central metal.[27] Because of increased catecholate oxygen atom to metal π-interaction in trigonal prismatic complexes, the change from an octahedral to a trigonal prismatic geometry has a dramatic influence on the energy and the intensity of the ligand to metal charge transfer (LMCT) transitions.[13,17,27] Although the spectra of Ga^{3+} (d^{10}), and Ti^{4+} (d^0) complexes (maximum at λ = 399, **15**; 397 nm, **16**) are not particularly useful, the Fe^{3+} (**10**, **11**) and V^{4+} compounds (**12**−**14**) have informative spectra. The absorption spectra of [Fe(bicappedTPTTRENCAM)]$^{3-}$ (**10**), [Fe(TPTCAM)]$^{3-}$ (**11**), [V(bicappedTRENCAM)]$^{2-}$ (**19**), [V(bicappedTPTTRENCAM)]$^{2-}$ (**12**), [V(bicappedTPTCAM)]$^{2-}$ (**13**), and [V(ETA)$_3$]$^{2-}$ (**20**) in aqueous solution at pH = 7 are presented in Figure 1.

In the iron(III) complexes **10** and **11**, the bands at about 363 nm and 335 nm, respectively, arise from ligand (π−π*) transitions. The two transitions at lower energy are assigned to ligand to metal charge transfer (LMCT) transitions.[28,29] Previous work has shown that the transition at about 510 nm in these systems varies only slightly in changing from octahedral to trigonal prismatic geometry.[27] However, the higher energy LMCT band is somewhat indicative of the geometry around iron. In the spectrum of [Fe(bicappedTPTTRENCAM)]$^{3-}$ (**10**), the band at 444 nm (ϵ = 4900) is very typical for pseudo-octahedrally coordinated iron(III) tris(2,3-dihydroxyterephthalamide) compounds.[13] In the trigonal prismatic compound [Fe(bicappedTRENCAM)]$^{3-}$ (**21**) this transition is observed at higher energy, with a larger extinction coefficient (428 nm, ϵ = 7200 M^{-1} cm^{-1}) due to a larger degree of π bonding.[13] The spectrum of [Fe(TPTCAM)]$^{3-}$ (**11**) with a LMCT transition at

(19) In solution with low concentration of H_6-bicappedTRENCAM·2HBr (**2**), only the mono-HBr salt can be observed which shows no mirror plane perpendicular to the terephthal units (compare with ref 13). Only a high concentration of **2** allows the detection of the bis-HBr adduct.

(20) See for [Fe(O$_2$C$_6$H$_4$)$_3$]$^{3-}$: Raymond, K. N.; Isied, S. S.; Brown, L. D.; Fronczek, F. R.; Nibert, J. H. *J. Am. Chem. Soc.* **1976**, *98*, 1767.
(21) See for [V(O$_2$C$_6$H$_4$)$_3$]$^{2-}$: Cooper, S. R.; Koh, Y. B.; Raymond, K. N. *J. Am. Chem. Soc.* **1982**, *104*, 5092.
(22) See for [Ti(O$_2$C$_6$H$_4$)$_3$]$^{2-}$: Borgias, B. A.; Cooper, S. R.; Koh, Y. B.; Raymond, K. N. *Inorg. Chem.* **1984**, *23*, 1009.
(23) See for [Ga(O$_2$C$_6$H$_4$)$_3$]$^{3-}$: Borgias, B. A.; Barclay, S. J.; Raymond, K. N. *J. Coord. Chem.* **1986**, *15*, 109.
(24) Hesse, M.; Meier, H.; Zeeh, B. *Spektroskopische Methoden in der organischen Chemie*; Georg Thieme Verlag: Stuttgart, New York, 1984; p 172.
(25) Bulls, A. R.; Pippin, C. G.; Hahn, F. E.; Raymond, K. N. *J. Am. Chem. Soc.* **1990**, *112*, 2627.
(26) Karpishin, T. B.; Stack, T. D. P.; Raymond, K. N. *J. Am. Chem. Soc.* **1993**, *115*, 6115.
(27) Karpishin, T. B.; Gebhard, M. S.; Solomon, E. I.; Raymond, K. N. *J. Am. Chem. Soc.* **1991**, *113*, 2977.
(28) Garrett, T. M. Ph.D. Thesis, University of California, Berkeley, 1988.
(29) Garrett, T. M.; Cass, M. E.; Raymond, K. N. *J. Coord. Chem.* **1992**, *25*, 241.
(30) For rare examples of homoleptic molybdenum catechol complexes see: (a) Pierpont, C. G.; Buchanan, R. M. *J. Am. Chem. Soc.* **1975**, *97*, 4912. (b) Cass, M. E.; Pierpont, C. G. *Inorg. Chem.* **1986**, *25*, 123. (c) Pierpont, C. G.; Downs, H. H. *J. Am. Chem. Soc.* **1975**, *97*, 2123.

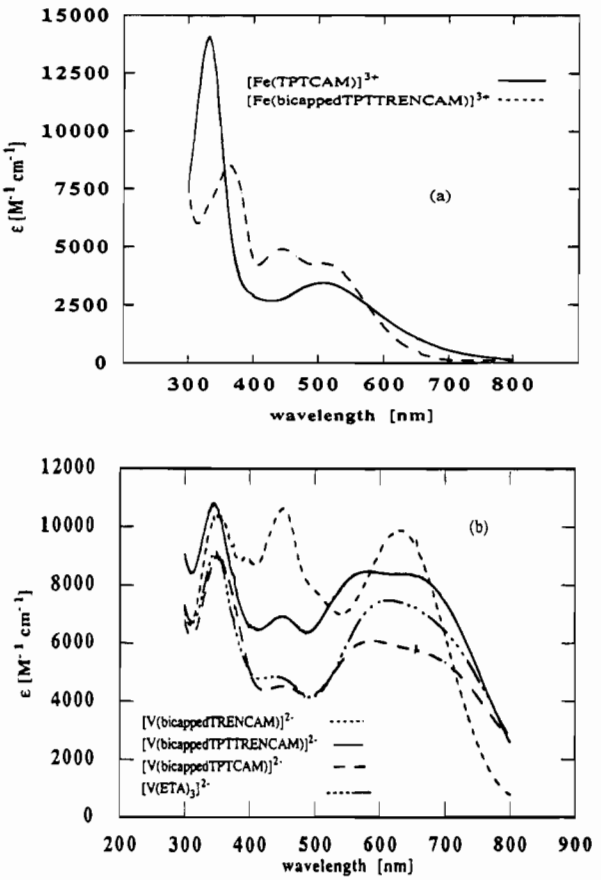

Figure 1. UV−visible spectra of (a) **10** and **11**, and (b) **19**, **12**, **13**, and **20**.

494 nm is very similar to that described for the octahedral complex $[Fe(TRENCAM)]^{3-}$ (**22**).[10]

The spectra of the vanadium compounds presented here have been assigned by analogy to the four characterized transitions observed for $[V(enterobactin)]^{2-}$ (**23**).[17] These compounds exhibit a ligand ($\pi-\pi^*$) transition at about 350 nm, and LMCT transitions at lower energy (between 400 and 800 nm). In the green trigonal prismatic complex $[V(bicappedTRENCAM)]^{2-}$ (**19**), two absorptions with high extinction coefficients are observed at 450 and 630 nm (ϵ = 10500 and 9400 $M^{-1}cm^{-1}$, respectively). The transitions of the dark blue octahedral complex $[V(ETA)_3]^{2-}$ (**20**),[16] on the other hand, show lower extinction coefficients, especially for the transition at about 440 nm; $[V(bicappedTPTTRENCAM)]^{2-}$ (**12**), $[V(bicappedTPTCAM)]^{2-}$ (**13**), and $[V(TPTCAM)]^{2-}$ (**14**) (not shown) have spectra and color very similar to that of $[V(ETA)_3]^{2-}$ (**20**), indicating that those compounds also are essentially octahedral at the metal center.

Voltammetric Measurements of the V(IV) Compounds. Cyclicvoltammetric investigations of iron(III) complexes with the ligands **2**−**4** are described elsewhere.[12] The electrochemistry of the complexes $[V(ETA)_3]^{2-}$ (**20**), $[V(TPTCAM)]^{2-}$ (**14**), $[V(bicappedTRENCAM)]^{2-}$ (**19**), $[V(bicappedTPTTRENCAM)]^{2-}$ (**12**), and $[V(bicappedTPTCAM)]^{2-}$ (**13**) were investigated in 0.1 M Bu_4NPF_6/DMF containing about 0.1 mmol of metal complex. The cyclic voltammograms in which the waves are assigned to the $V^{V/IV}$ redox potential are shown in Figure 2 and Table 2. A quasi-reversible wave at +0.28 V is observed for $[V(TPTCAM)]^{2-}$ (**14**), which is typical for 2,3-dihydroxy benzamide complexes.[17] The waves of $[V(bicappedTRENCAM)]^{2-}$ (**19**) (+ 0.67 V) and $[V(bicappedTPTTRENCAM)]^{2-}$ (**12**) (+ 0.64 V) are essentially reversible, whereas $[V(bicappedTPTCAM)]^{2-}$ (**13**) shows an irreversible potential of +0.66 V (current ratio = 2.16) and a second oxidation step at +0.99 V. Similar redox properties can be detected for $[V(ETA)_3]^{2-}$ (**20**) (oxidations at +0.72 and +0.90 V, reduction at +0.15 V). This irreversible behavior may be due to dissociation of one of the three ligands. The increased potential of the bisamide ligands compared to monoamide ligands such as **14** shows that these ligand systems stabilize the V(IV) oxidation state relative to V(V). This is consistent with the less basic character of the bisamide catecholate oxygen atoms compared to the monoamide ligands, and appears to lead to dissociation of the V(V) compounds with flexible ligands like **4** or **6**.

Table 2. Redox Potential, Peak Separation, and Current Ratio Observed for the Vanadium Compounds **12**−**14**, **19**, and **20** (DMF vs SCE)[a]

	redox potential $V^{V/IV}$ (V)	peak separation (mV)	current ratio
$[V(TPTCAM)]^{2-}$ (**14**)	+0.28	71	1.18
$[V(bicappedTRENCAM)]^{2-}$ (**19**)	+0.67	78	1.10
$[V(bicappedTPTTRENCAM)]^{2-}$ (**12**)	+0.64	88	1.24
$[V(bicappedTPTCAM)]^{2-}$ (**13**)	+0.66 [+0.99 (ox.)]	95	2.16
$[V(ETA)_3]^{2-}$ (**20**)	+0.72 (ox.) +0.90 (ox.) +0.15 (red.)		

[a] Conditions: ca. 0.1 mM metal complex concentration, 0.1 M Bu_4NPF_6, Pt working electrode, 0.1 V/s.

Scheme 3

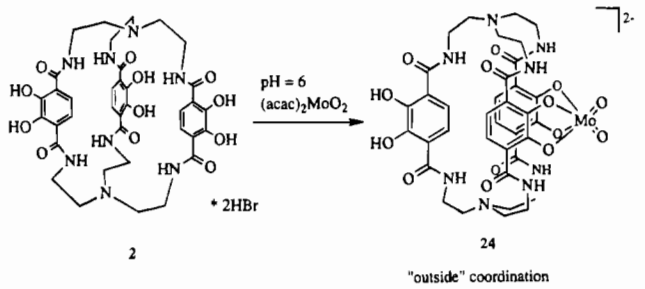

The quasi-reversible redox behavior of compounds **14**, **19**, and **12**, in contrast to the behavior of **13** and **20**, is also reflected in the air sensitivity of water solutions of the complexes. Dark blue solutions of **13** or **20** decolorize within a few days (7 days or 1 day, respectively), whereas solutions of **12**, **14**, or **19** show no change in color over a period of several weeks.

Spectroscopic Features of 24. A spectroscopic analysis of $[(H_2\text{-bicappedTRENCAM})MoO_2]^{2-}$ (**24**) shows the MoO_2 unit has the usual cis geometry. The typical vibrational frequencies for a *cis*-MoO_2 unit are found in the IR spectrum of **24** at 899 and 863 cm^{-1}; $Na_2[(BTA)_2MoO_2]$ (**25**) exhibits nearly the same Mo−O bands at 899 and 864 cm^{-1}.[31]

Two different sets of signals for the ligand 2,3-dihydroxy terephthalamide moieties are observed in the ^1H NMR spectrum of **24** in dmso-d_6 (Figure 3, Table 1). The signals occur in a 2:1 integration ratio. The difference in the two sets' aromatic and amide proton chemical shifts, as well as the shifts of the two hydroxo group protons (2H at 12.28 ppm), indicate the presence of two coordinated and one uncoordinated, protonated catecholate unit. The catechol H_{aryl} (6.70 ppm) and H_{amide} (9.27 ppm) protons of the larger set occur in the shift regions typical for coordinated catechol groups, and are very similar to the shifts seen in the spectrum of **25** (6.95 (H_{aryl}) and 9.19 ppm (H_{amide})).

(31) Griffith, W. P.; Pumphrey, C. A.; Rainey, T.-A. *J. Chem. Soc., Dalton Trans.* **1986**, 1125.

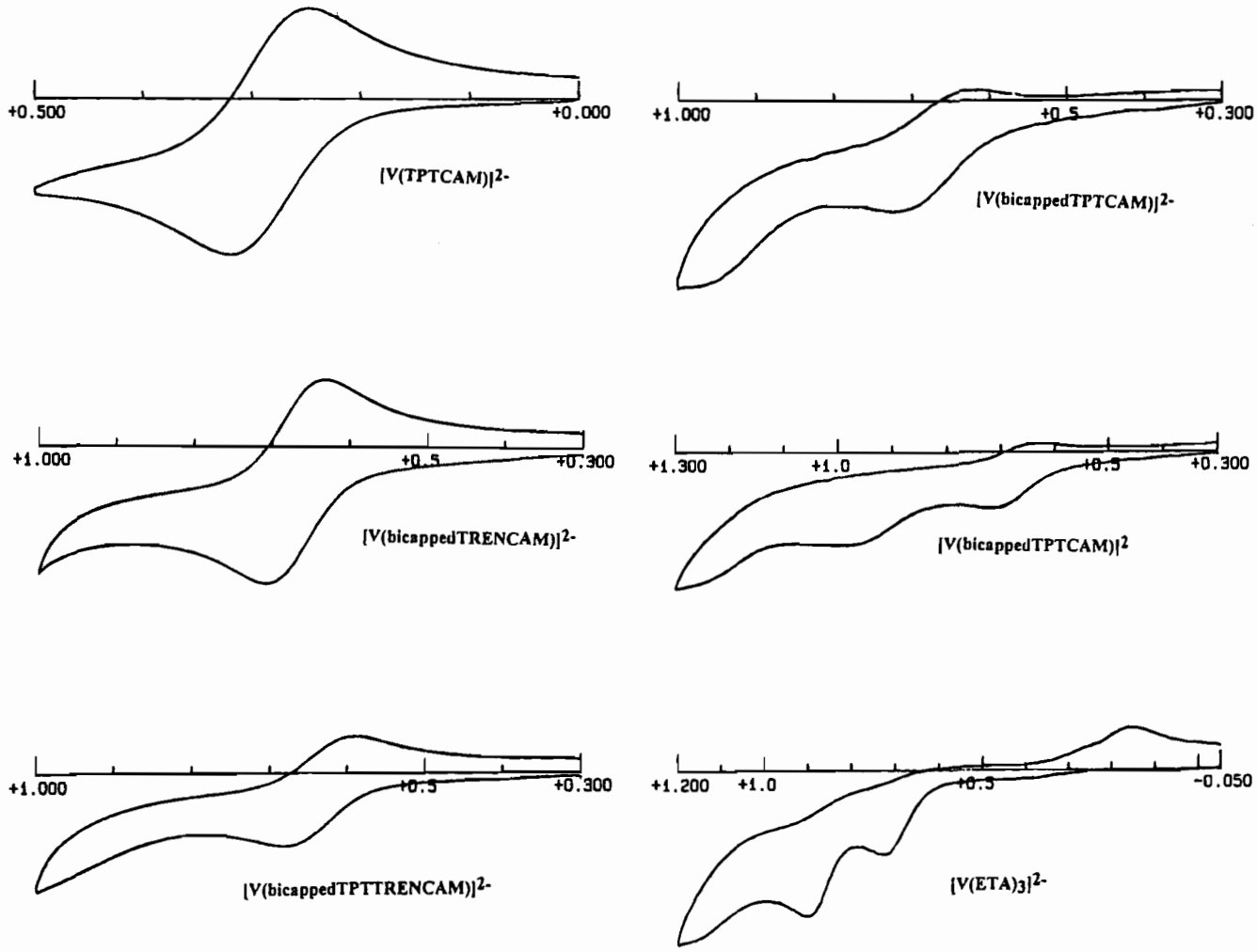

Figure 2. Cyclic voltammograms of the vanadium complexes **14**, **19**, **12**, **13**, and **20** in DMF vs SCE. Conditions: ca. 0.1 mM metal complex concentration, 0.1 M Bu_4NPF_6, Pt working electrode, 0.1 V/s.

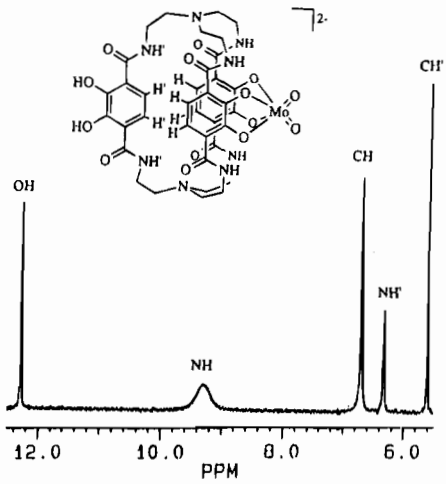

Figure 3. Section of the ^1H NMR spectrum of **24** in dmso-d_6 presenting the signals of the aromatic, amide, and hydroxy protons.

The H_{amide} shifts are in the region for amide protons forming hydrogen bridges.

For the uncoordinated terephthalamide of **24**, upfield shifts occur because of the anisotropic effect of the two coordinated terephthalamides aromatic rings influencing the shielding of the protons situated between those two rings. The amide protons appear at 6.33 ppm and the aromatic protons at 5.61 ppm (5.25 ppm in D_2O!). This is evidence that the aromatic and the amide protons of the uncoordinated catecholamide point into the interior of the cavity of the macrobicyclic molecule. The hydroxo functionalities and the amide oxygen atoms, however, are directed away from the macrocycle, and the *cis*-MoO_2 unit is coordinated to the "outside" of the cage molecule.

X-ray Crystal Structure of K_2[(H_2-bicappedTRENCAM)-MoO_2] (24′). X-ray quality crystals of **24′** were obtained by diffusion of ether into wet DMF (approximately 5−10% water). Although elemental analysis shows that the bulk sample **24** was obtained as the disodium salt, X-ray diffraction established that the cation in the crystal selected from the bulk sample was potassium, introduced in the initial step of the synthesis in which KOH was used for deprotonation. The potassium salt **24′** crystallizes in the monoclinic space group $P2_1/c$ (No. 14) with cell parameters described in Table 4.

The X-ray structure nicely elucidates the general features of the dianion [(H_2-bicappedTRENCAM)MoO_2]$^{2-}$ (Figure 4, Table 3) although the cations and the various solvent molecules (five water, one DMF) show some disorder. The MoO_6 unit possesses a distorted octahedral geometry with the two double bonded oxygen atoms oriented *cis* to each other (d(Mo=O) = 1.722(7), and 1.709(8) Å; O=Mo=O = 99.1(4)°). This *cis*-MoO_2 unit is coordinated "outside" of the cavity of the macrobicyclic molecule as was expected based on spectroscopic data. One of the two oxygen atoms of this unit is within hydrogen bonding distance of a water molecule (d(O··O) = 2.856 Å).[32] Further hydrogen bonding seems to occur between the amide and catecholate functionalities of the coordinated units. The observed geometry is typical for dicatechol molyb-

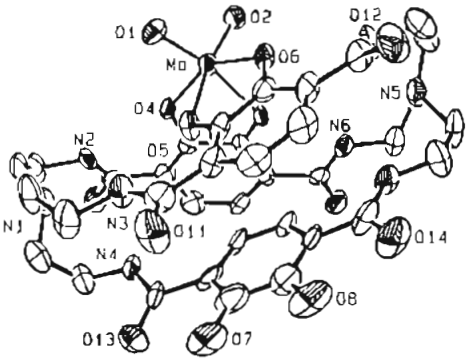

Figure 4. Molecular structure of the dianion $[(H_2\text{-bicappedTRENCAM})MoO_2]^{2-}$.

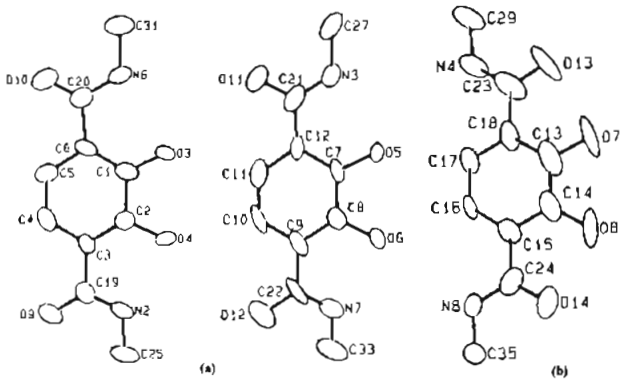

Figure 5. Presentation of (a) the two coordinating, and (b) the noncoordinating 2,3-dihydroxy terephthal amide units of **24**.

Table 3. Selected Bond Lengths (Å) and Angles (deg) for **24′**

Mo−O1 1.722(7)	O1−Mo−O2 99.14(4)
Mo−O2 1.709(8)	
Mo−O3 2.176(7)	O3−Mo−O4 74.3(3)
Mo−O4 1.997(8)	O5−Mo−O6 74.8(3)
Mo−O5 2.167(7)	
Mo−O6 1.991(7)	

denum dioxo dianions.[33-35] The uncoordinated dihydroxyterephthalediamide moiety of **24′** is oriented parallel to one of the coordinated units (π stacking) with the aromatic and the amide protons pointing towards the π system of the third aromatic group. This is evidenced in solution by the anisotropic shift in the ^{1}H NMR spectrum.

Compound **24′** gives the opportunity to compare coordinated and uncoordinated 2,3-dihydroxyterephthalamide units in one molecule. Both of these units are nearly planar, with slight distortions due to the strain of the macrobicyclic molecule. Figure 5a presents the two coordinating moieties. The nitrogen atoms of the amide groups are oriented in the same direction as the catecholate oxygen atoms, allowing hydrogen bonding between these two functionalities (d(O···N) = 2.699, 2.702, or 2.708, 2.732 Å). In contrast to this conformation, the uncoordinated unit is rotated approximately 180° about the $C_{amide}-C_{aromatic}$ bonds (Figure 5b). This leads to an orientation of the four oxygen atoms (two catechol, two amide) in the same direction, allowing hydrogen bridging between catechol and amide oxygen atoms (d(O···O) = 2.551 and 2.510 Å). This conformational difference between coordinated and uncoordinated catecholamide ligands has been observed earlier in X-ray studies of free ligands and their metal complexes, even those not constrained by macrocyclic structures.[12,13,26,29]

Table 4. Summary of Crystal Data for $K_2(H_2\text{-bicappedTRENCAM})MoO_2]$ (**24′**)

formula:	$C_{39}H_{51}MoN_9O_{20}$
fw	1142.01
temp (°C)	−90
crystal system	triclinic
space group	$P2_1/c$ (No. 14)
cell consts[a]	
a (Å)	13.322(2)
b (Å)	14.252(2)
c (Å)	27.885(3)
α (deg)	90
β (deg)	103.11(1)
γ (deg)	90
Z	4
V (Å^3)	5156.7(2.6)
abs coeff, μ_{calc} (cm^{-1})	4.86
δ_{calc} (g/mL)	1.471
F(000)	2360
cryst dimens	0.25 × 0.25 × 0.10 mm
radiation	Mo Kα (λ = 0.71073 Å)
diffractometer	Enraf-Nonius CAD-4
h,k,l range collctd	0 → 14, −15 → 15, −30 → 30
2θ range	3.0−45.0°
scan type	$\theta-2\theta$
scan speed (θ, deg/min)	5.49
no. of reflcns collcd	8492
no. of unique reflcns	6743
no. of reflcns with ($F_o^2 > 3^*\sigma(F_o^2)$)	3272
no. of paramrs	701
data/param ratio	4.7
$R = [\sum\|\Delta F\|/\sum\|F_o\|]$	0.064
$R_w = [\sum w(\Delta F)^2/\sum wF_o^2]$	0.072
GOF	1.634
final diff $\rho_{max}{}^+/\rho_{max}{}^-$ (e$^-$/Å^3)	+0.629[b]/−0.165[c]

[a] Unit cell parameters and their esd's were derived by a least-squares fitting of the setting angles of 24 reflections in the range 23.728° ≤ 2θ ≤ 24.610°. [b] Located near K2 fragments. [c] Located near K2 fragments. An empirical absorption correction (EAC) was applied based on azimuthal scans: min(av) = 86.1%.

Conclusions

Macrobicyclic triscatecholate siderophore analogs are versatile in their ability to bind a variety of main group, 3d, and 4d metal ions. However, choice of backbones allows a fine tuning of the cage molecule's cavity size, which consequently influences metal coordination geometry. As shown earlier, the smallest ligand bicappedTRENCAM (**2**) is capable of enforcing an unusual trigonal-prismatic geometry at 3d metal centers.[12,13] This is due to very tight ligand to metal interactions overcoming the ligand-ligand repulsion which is relatively larger in trigonal-prismatic geometry than pseudo-octahedral geometry. As indicated by UV−visible spectroscopy, the somewhat larger bicappedTPTTRENCAM (**3**), as well as the largest ligand investigated here, bicappedTPTCAM (**4**), form pseudo-octahedral coordination compounds with Fe^{3+} or V^{4+}.

Cyclic voltammetry (CV) investigations of the vanadium compounds have been presented and compared to the vanadium complexes of the new ligand TPTCAM (**5**), and of ETA (**6a**). The CV measurements show that the terephthalamide ligands **2**−**4**, and **6a** are relatively better at stabilizing vanadium in the 4+ oxidation state than analogous benzamide derivatives like TPTCAM (**5**). The macrobicyclic ligand cavity size is found to have a great influence on the reversibility of the oxidation

(32) See for a comparison: Haselhorst, G.; Stotzel, S.; Strassburger, A.; Walz, W.; Wieghardt, K.; Nuber, B. *J. Chem. Soc. Dalton Trans.* **1993**, 83.

(33) Yamanouchi, K.; Enemark, J. H. in *Third International Conference on Molybdenum Chemistry*; Barry, H. F., Mitchell, P. C. H., Eds.; Climax: New York, 1979; p 24.

(34) Pierpont, C. G.; Buchanan, R. M. *Coord. Chem. Rev.* **1981**, *38*, 45 and literature cited therein.

(35) Dowerah, D.; Spence, J. T.; Singh, R.; Wedd, A. G.; Wilson, G. L.; Farchione, F.; Enemark, J. H.; Kristofzski, J.; Bruck, M. *J. Am. Chem. Soc.* **1987**, *109*, 5655.

of the vanadium(IV) compounds. Unlike complex **4**, which shows irreversible behavior very similar to that observed for the tris-ETA complex (**20**), the two smallest ligands (**2**,**3**) show reversible CV waves. This indicates the relatively tighter encapsulation of the oxidized cation prevents further reaction of the V^{5+} compounds. The terephthalamide units of bicappedTPTCAM (**4**) apparently act as three independent bidentate ligands, although they are connected by two large and flexible backbones.

Unlike the other metal ions described here, the larger, nonspherical complex cation *cis*-MoO_2^{2+} cannot be fully incorporated into the bicappedTRENCAM (**2**) cavity. Rather, the cation is coordinated to the "outside" of the macrobicyclic cage, as the crystal structure of **24′**, which reveals the geometry of the dianion $[(H_2\text{-bicappedTRENCAM})MoO_2]^{2-}$, nicely shows. The observed structure of **24′** is the first where a *cis*-MoO_2 unit is coordinated to a siderophore analog. Naturally occurring siderophores are well known to have an important part in the regulation of the uptake and transport of iron(III), and probably of other biorelevant metals. In this context, structures like that of **24′** have been proposed to be important regulators in the transport of molybdenum(VI) in organisms.[36,37]

Acknowledgment. We thank Dr. Frederick J. Hollander for his help with the crystallography. This research was supported by the National Institute of Health, Grants AI 11744 and, in part, DK 32999. M.A. gratefully acknowledges a NATO postdoctoral fellowship.

Supplementary Material Available: X-ray crystallographic data for $K_2[(H_2\text{-bicappedTRENCAM})MoO_2]$ (**24′**), including tables of anisotropic thermal parameters, atom positional parameters, and nonessential inter- and intramolecular distances and angles (7 pages). Ordering information is given on any current masthead page.

(36) Hider, R. C. *Struct. Bonding* **1984**, *58*, 26.
(37) Wilshire, J. P.; Leon, L.; Bosserman, P.; Sawyer, D. T.; Buchanan, R. M.; Pierpont, C. G. In *Third International Conference on Molybdenum Chemistry*; Barry, H. F., Mitchell, P. C. H., Eds.; Climax: New York, 1979; p 264.